Research Square

Preprints are preliminary reports that have not undergone peer review.
They should not be considered conclusive, used to inform clinical practice,
or referenced by the media as validated information.

Retrieval of wheat biophysical parameters using hybrid polarimetric SAR decompositions from RISAT-1 data

Dipanwita Haldar[1]
[1]Indian Institute of Remote Sensing, Indian Space Research Organisation (ISRO)
Gopal Kumar[2]
g.kumar@cgiar.org

International Water Management Institute, India
Rucha Dave[3]
Anand Agricultural University
Viral Dave
Dhirubhai Ambani Institute of Information and Communication Technology
Arundhati Misra
Space Applications Centre

Research Article

Keywords: hybrid polarimetric SAR, wheat biomass, RISAT-1, decomposition, crop monitoring

Posted Date: November 5th, 2026

DOI: https://doi.org/10.21203/rs.3.rs-10642086/v1

License: This work is licensed under a Creative Commons Attribution 4.0 International License.
Read Full License

Additional Declarations: No competing interests reported.

Retrieval of wheat biophysical parameters using hybrid polarimetric SAR decompositions from RISAT-1 data

Dipanwita Haldar[1], Gopal Kumar[2]*, Rucha Dave[3], Viral Dave[4], Arundhati Misra[5]

[1]Indian Institute of Remote Sensing, Indian Space Research Organisation (ISRO), Dehradun 248001, Uttarakhand, India
[2]International Water Management Institute, New Delhi 110012, India
[3]Anand Agricultural University, Anand, Gujarat, India
[4]Dhirubhai Ambani Institute of Information and Communication Technology, Gujarat, India
[5]Space Application Centre (ISRO), Ahmedabad

Corresponding author
Name: Gopal Kumar
Email id: g.kumar@cgiar.org
ORCID ID (Gopal Kumar): 0000-0003-3036-1619

Acknowledgement
The authors thank their colleagues at the Space Applications Centre, ISRO, Ahmedabad, for technical discussions and support during field data collection and data processing. The authors also acknowledge the use of the PolSARpro software and in-house processing tools for hybrid polarimetric analysis.

Author Contributions
Conceptualization: Dipanwita Haldar and Gopal Kumar; methodology and data analysis: Dipanwita Haldar, Gopal Kumar, Rucha Dave and Viral Dave; field investigation: Dipanwita Haldar, Rucha Dave and Viral Dave; supervision: R. P. Singh and Arundhati Misra; writing: original draft: Dipanwita Haldar and Gopal Kumar; writing—review and editing: all authors. All authors read and approved of the final manuscript.

Abstract
Accurate estimation of crop biophysical parameters such as biomass and phenological stage is critical for large-scale agricultural monitoring. Synthetic Aperture Radar (SAR), particularly in hybrid polarimetric mode, offers enhanced capability for vegetation characterization under all-weather conditions. This study investigates the retrieval of wheat biophysical parameters using hybrid polarimetric decomposition techniques applied to RISAT-1 C-band SAR data acquired during the 2015–2016 rabi season over Junagadh district, Gujarat, India. Ground-based measurements, including crop biomass and age, were collected in synchronization with satellite overpasses. Stokes parameter-based decompositions, m-δ and m-χ, were implemented alongside Raney decomposition to examine their sensitivity to biomass, crop growth progression, and maturity. Additionally, the Radar Vegetation Index and Alpha Angle were derived from C2 and pseudo-C3 matrices to assess their correlation with ground-truth parameters. Results indicate that the m-δ decomposition provides the most consistent response, with odd-bounce components decreasing and diffuse scattering increasing as biomass and crop age progress. Radar Vegetation Index values ranged from 0.27 to 0.52, while Alpha Angle values indicated a transition from surface to volume scattering with crop development. The diffuse component of the m-δ decomposition showed the strongest correlation with field-measured biomass, outperforming both m-χ and Raney methods. The study confirms the effectiveness of hybrid polarimetric SAR for estimating crop biophysical parameters and presents a transferable decomposition framework for operational crop monitoring. The findings are directly applicable to national and global agricultural monitoring programmes and provide methodological benchmarks for hybrid SAR missions, including RISAT-1A/1B and NISAR.

Keywords: hybrid polarimetric SAR; wheat biomass; RISAT-1; decomposition; crop monitoring.

1. **Introduction**

Timely and accurate estimation of crop biophysical parameters such as above-ground biomass and phenological stage is crucial for precision agriculture, yield modeling, irrigation scheduling, and food security forecasting. Remote sensing has emerged as an indispensable tool in this context, providing spatially and temporally continuous crop information at multiple scales utilizing various resolutions. While optical sensors have traditionally dominated agricultural applications due to their spectral richness, they suffer from significant limitations under cloudy or hazy conditions, especially during critical crop growth stages. Synthetic Aperture Radar (SAR), with its ability to acquire data regardless of weather or illumination conditions, offers a robust alternative (McNairn and Shang 2016).

SAR signals interact with vegetation and soil through scattering mechanisms that are influenced by surface roughness, dielectric properties, and canopy structure. This makes SAR particularly sensitive to crop biophysical variables such as biomass, moisture content, and canopy architecture (Veloso et al. 2017; Skriver et al. 1999). Consequently, SAR has been increasingly used for land cover classification (Inglada et al. 2017), phenological monitoring (Song et al. 2021), and biomass estimation (Vreugdenhil et al. 2018), particularly in cloud-prone and haze-affected regions, including the subtropics, which continue to serve as major global food production zones.

Among the different SAR acquisition modes, full polarimetric SAR (Quad-Pol) provides the most comprehensive scattering information. However, it comes at the cost of reduced swath width and

temporal frequency. Dual-polarimetric SAR offers broader coverage but with limited scattering characterization. Hybrid polarimetric SAR, which transmits a circularly polarized wave and receives two orthogonal linear polarizations, provides a balanced trade-off between information content and operational efficiency (Raney 2007a). By capturing coherent backscatters in two orthogonal channels (e.g. RH and RV) along with phase information, hybrid SAR allows the computation of all four Stokes parameters, enabling advanced polarimetric decomposition without requiring a full polarimetric system (Raney 2016).

Hybrid polarimetric SAR has gained renewed attention following the launch of RISAT-1A by the Indian Space Research Organisation in 2022, which reintroduces the hybrid mode with improved revisit and resolution capabilities (ISRO 2025). Several projects are currently underway, and few have matured across different regions of India including national and global monitoring to evaluate its applicability for agricultural monitoring and related applications. However, detailed analyses utilizing hybrid SAR for agricultural parameter retrieval remain sparse, particularly with respect to erectophile crops like wheat. Wheat presents a vertical canopy structure with upright leaves and stems, leading to unique scattering behavior distinct from planophile crops such as mustard, soybean, or cotton (Thota et al. 2015).

Past studies have demonstrated the utility of SAR for vegetation characterization using various decomposition techniques. For instance, Freeman–Durden, Cloude–Pottier, and Yamaguchi decompositions have been widely employed for forest and crop classification (Freeman and Durden 1998; Cloude and Pottier 1997). However, these have been predominantly applied using full-polarimetric data. With the increasing availability of hybrid SAR systems, there is a need to evaluate decomposition methods specifically tailored to Stokes parameters such as the m-δ (delta) and m-χ (chi) decompositions as proposed by recent advancements in hybrid scattering theory (Raney 2007b; Charbonneau et al. 2010).

Although studies have explored hybrid SAR applications for general land cover mapping and rice crop classification (Singha and Swain 2023), few have focused on quantifying the sensitivity of hybrid-mode decompositions to biophysical parameters such as biomass and crop age. Moreover, comprehensive validation of decomposition outputs with field-measured parameters for wheat is notably lacking in the literature. This gap is critical, as wheat constitutes a major staple crop globally, and its monitoring is vital for food policy planning and market regulation (FAO 2025).

This study addresses the above knowledge gap by applying hybrid SAR decomposition techniques to estimate wheat biophysical parameters using RISAT-1 C-band data. The analysis was conducted for the 2015–2016 rabi season over Junagadh district in Gujarat, India, a region characterized by intensive, yet non-conventional and short-duration (about 100 days), wheat cultivation. The early onset of summer in this region provides a relevant agroclimatic setting for examining crop growth dynamics under increasing climate variability. Ground truth data comprising wheat biomass and crop age were collected in close synchrony with RISAT-1 satellite overpasses to support validation. Three hybrid polarimetric decomposition techniques including m-δ, m-χ based on Stokes parameters, along with Raney decomposition, were evaluated to investigate their sensitivity to wheat biophysical parameters.

The novelty of this study lies in (i) systematic comparison of multiple hybrid-mode decompositions in relation to field-measured wheat biophysical parameters, (ii) establishing the relative sensitivity of decomposition components to biophysical variations across phenological stages, and (iii) providing a transferable framework that can be applied to RISAT-1A, NISAR, and other hybrid SAR missions for operational crop monitoring.

The outcomes are relevant not only for SAR remote sensing research but also for agencies involved in agricultural assessment, crop insurance, and food security monitoring. By validating hybrid-mode

capabilities for biophysical retrieval in erectophile crops, this study contributes toward bridging the methodological gap and advancing the application potential of upcoming hybrid and full-polarimetric SAR missions.

2. Study area and data

2.1 Study Area

The study was conducted in the Junagadh district of Gujarat, India, within a 25 km × 25 km region centered around Keshod city at 21°10′N to 21°30′N latitude and 70°09′E to 70°30′E longitude (Fig. 1). This region is a major wheat-growing zone in Gujarat State during the rabi season (Nov- Feb) with short growing season and is characterized by a semi-arid monsoon climate with an average annual rainfall of approximately 800 mm, primarily received during the kharif season (June - Oct). The landscape is predominantly composed of irrigated agricultural land, interspersed with orchards (comprising mainly mango and sapodilla), natural vegetation, scrublands, villages, and small urban settlements. Wheat is the dominant rabi crop, with supplementary cropping of coriander, cumin, and gram depending on irrigation availability. The area was selected due to its high crop density including early maturing wheat, spatial variability in field conditions, and logistical feasibility for ground surveys.

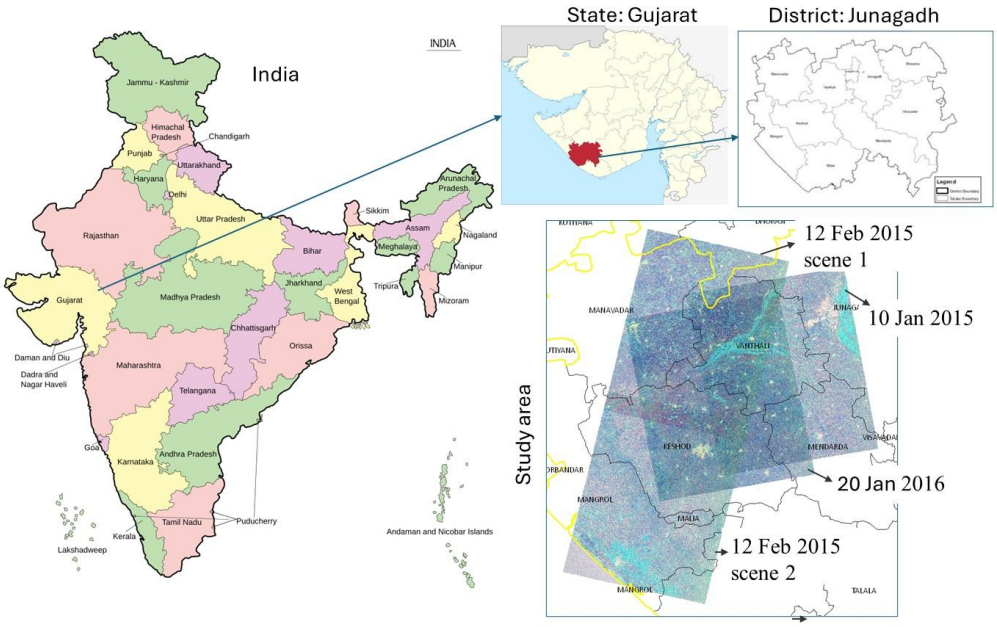


Fig. 1. Location map of the study area in Junagadh district, Gujarat, showing major land use categories and RISAT-1 acquisition footprints.

2.2 Satellite Data

Hybrid polarimetric SAR data from the C-band RISAT-1 satellite were used in this study (Table 1). The data were acquired in Fine Resolution Stripmap (FRS) mode at a spatial resolution of approximately 1.8 m with Single Look Complex (SLC) format. Four scenes were selected across two rabi seasons: January–February 2015 and January 2016, covering key crop growth stages from tillering to maturity.

Table 1. RISAT-1 hybrid/compact-pol SAR acquisition details.

Acquisition Date	Scene Center Coordinates (Lat, Lon)	Incidence Angle (°)	Orbit Direction (node)	Polarization Mode
10 Jan 2015	21.42°N, 70.38°E	41.61	Ascending	RH, RV
12 Feb 2015 (S1)	21.48°N, 70.24°E	45.24	Descending	RH, RV
12 Feb 2015 (S2)	21.22°N, 70.18°E	45.24	Descending	RH, RV
20 Jan 2016	21.40°N, 70.28°E	40.91	Ascending	RH, RV

The combination of ascending and descending orbits allowed partial multi-temporal observation, although some ground reference points were missed due to differences in viewing geometry.

2.3 Ground Data Collection

Ground truth (GT) campaigns were conducted in close synchrony with satellite overpasses, ensuring temporal consistency with SAR data acquisition (Fig. 2). Field surveys were carried out on 9 January and 13 February 2015, and again on 20–21 January 2016, aligning precisely with the respective RISAT-1 acquisition dates.

Each GT dataset included GPS-tagged observations of phenological stages and biomass (Fig. 3):

- Crop type
- Crop age (days after sowing)
- Crop height and phenological stage
- Above-ground biomass (measured from 1 m² quadrants)
- Leaf dimensions and vigor
- Soil moisture and surface roughness

Fields larger than 2 ha were prioritized for sampling to ensure SAR backscatter homogeneity. Other land cover types including bare soil, urban areas, water bodies, and orchards were also recorded for classification validation.

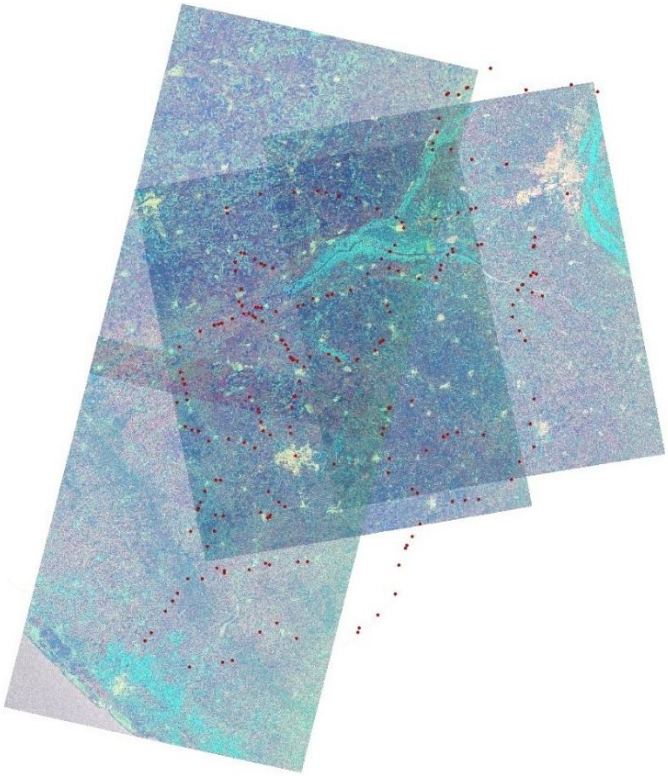


Fig. 2. Ground truth sample locations (dots) overlaid on RISAT-1 acquisition footprints.

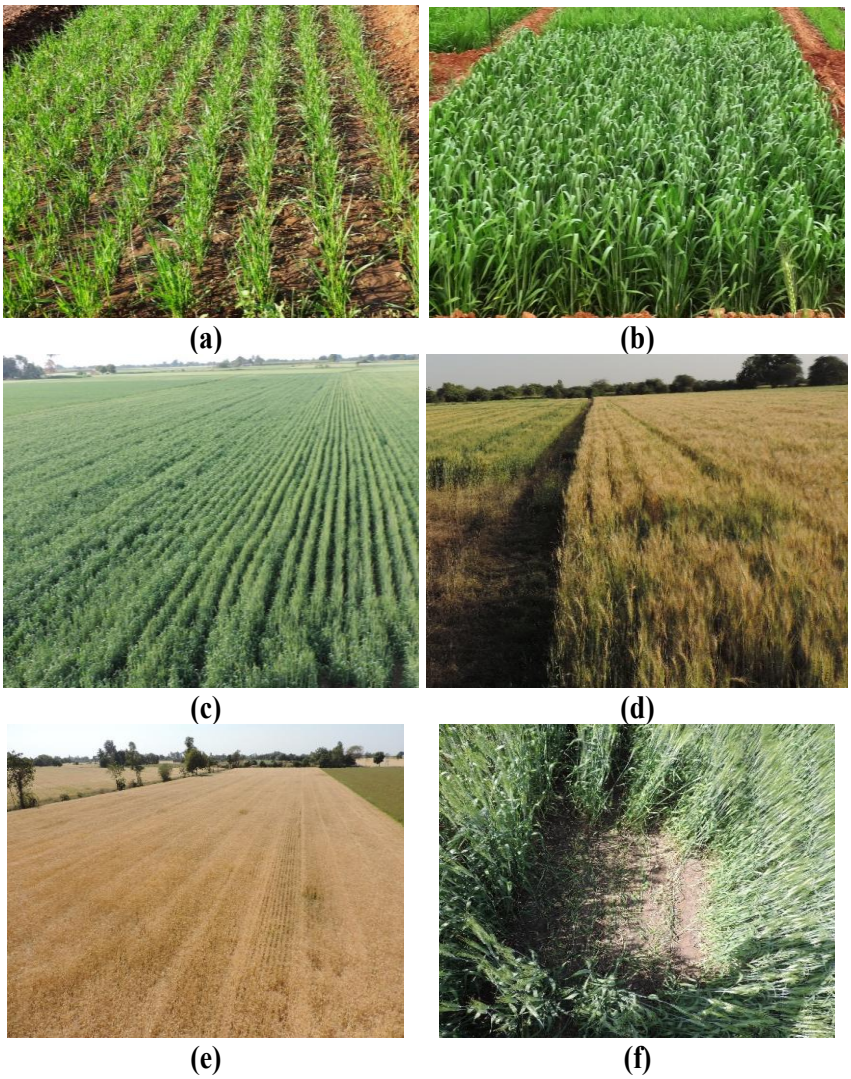


Fig. 3. Visual documentation of wheat crop phenological stages and biomass sampling procedure: (a) Initial establishment, (b) Tillering stage, (c) Flowering, (d) Dough stage, (e) Maturity, (f) Sampling biomass from 1 m² area.

2.4**.** Data Preprocessing and Software Tools

RISAT-1 hybrid SLC data were processed using a combination of in-house tools and the open-source PolSARpro v5.0 software suite. Preprocessing steps presented in Fig. 4. All datasets were co-registered to a common geographic grid using ground control points collected during field surveys.

2.5. Crop Grouping for Analysis

To enable statistical comparison, the field observations were categorized into three biomass groups: <2500 g/m², 2500–5000 g/m², >5000 g/m² and three age groups: <70 days, 70–105 days, >105 days (Table 2). This classification was used to evaluate the sensitivity of different SAR decomposition parameters and polarimetric indices across crop development stages.

Table 2. Summary of field data sample groups and their characteristics.

Category	Group Description	No. of Plots	Mean Biomass (g/m^2)	Mean Age (days)
Biomass Group 1	Low biomass (<2500)	28	~2100	~60
Biomass Group 2	Medium (2500–5000)	30	~3800	~85
Biomass Group 3	High (>5000)	18	~5400	~110
Age Group 1	Early (<70 days)	12	~3000	~60
Age Group 2	Mid (70–105 days)	10	~4000	~90
Age Group 3	Late (>105 days)	10	~5200	~110

3. Methodology

3.1 SAR Data Preprocessing

Preprocessing of RISAT-1 hybrid SAR data was performed using a combination of the open-source PolSARpro v5.0 software and a custom in-house Python-based toolset (MIDAS v. 2: vedas/sac.isro.in) optimized for hybrid data handling. The raw Single Look Complex (SLC) hybrid-mode data underwent the following steps (Fig. 4):

1. Radiometric Calibration: Applied to convert the digital numbers to radar backscatter coefficients (σ^0), ensuring comparability across acquisitions and incidence angles (Singha and Swain 2023).
2. Multilooking: A 3 × 3 look factor was applied to suppress speckles and improve radiometric stability while preserving spatial resolution suitable for field-scale analysis.
3. Geocoding and Terrain Correction: Image coordinates were converted to UTM projection using ground control points collected during field visits. Shuttle Radar Topography Mission (SRTM) DEM was used to correct terrain-induced distortions.
4. Stokes Parameter Derivation:The RH and RV channels were used to compute the four Stokes parameters (S_0, S_1, S_2, S_3), capturing the full information content of the hybrid polarimetric return (Raney 2007a; Raney 2007b)

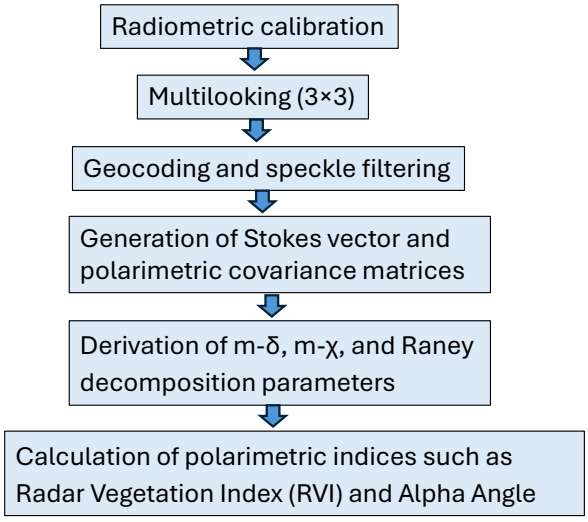


Fig. 4. Schematic diagram of preprocessing and decomposition workflow from SLC input to parameter extraction.

3.2 Polarimetric Decomposition Techniques

Polarimetric decomposition was carried out on the Stokes parameter dataset to extract physical scattering components. The following decompositions were applied:

3.2.1 m-δ (m-Delta) Decomposition

The m-δ decomposition utilizes the normalized Stokes parameters to isolate three primary scattering mechanisms: even-bounce (surface), odd-bounce (dihedral), and diffuse (volume) scattering. It is particularly suited for hybrid data as it avoids covariance matrix estimation (Raney 2007b; Charbonneau et al. 2010).

Let S = [S_0, S_1, S_2, S_3] be the normalized Stokes vector, then:

Even component

$$m_\delta^{even} = \frac{1+S_1}{2} \qquad \text{Eq.1}$$

Odd component

$$m_\delta^{odd} = \frac{1-S_1}{2} \qquad \text{Eq. 2}$$

Diffuse component

$$m_\delta^{diffuse} = \sqrt{S_2^2 + S_3^2} \qquad \text{Eq. 3}$$

3.2.2 m-χ (m-Chi) Decomposition

The m-χ decomposition offers a geometrical interpretation by using ellipticity and orientation of the polarization ellipse to characterize scattering components. Though less sensitive than m-δ in crop studies, it provides complementary insights (Raney 2024). The diffuse component, which is of primary interest in this study, is derived as complementary part of degree of polarization. The depolarized scattering contribution from the crop canopy, represented by (1 – m), remains consistent across both decomposition approaches.

Even and odd components: derived similarly using S_1, with alternative weighting to account for polarization ellipse tilt.

3.2.3 Raney Decomposition

Raney's hybrid decomposition, developed specifically for circular transmit / linear receive SAR systems, breaks the signal into even, odd, and ground components (Raney 2007a; Chirakkal et al. 2019). Though commonly applied in multilooked form, its sensitivity to crop biomass was compared against the full-resolution Stokes-based decompositions. All decomposition outputs were scaled between 0 and 1 and stored as thematic raster layers for further statistical analysis.

3.3 Vegetation Indices and Scattering Metrics

Two derived polarimetric indices were computed to support decomposition analysis:

3.3.1 Radar Vegetation Index (*RVI*)

RVI is a non-model-based index expressing vegetation density and vigor. For hybrid SAR, a modified form is used (Kim et al. 2012)

$$RVI = \frac{4 \cdot |S_2|}{S_0 + S_1} \qquad \text{Eq.4}$$

RVI values theoretically range between 0 (no vegetation) and 1 (dense vegetation) with few instances crossing 1.

3.3.2 Alpha Angle

Alpha Angle represents the average scattering mechanism and is derived via eigenvector analysis. In this study, alpha was estimated using both:

- C2 Matrix (2 × 2 covariance derived from RH and RV)
- Pseudo-C3 Matrix (approximation of full-pol C3 matrix from hybrid mode)

The alpha angle (α) ranges from:

0° → surface scattering

45° → volume scattering

90° → double bounce/dihedral scattering (Cloude and Pottier 1997; Haldar et al. 2016a)

These are near mean and ideal values, and the scatter/range is always found to be 10-15° around the mean for most of the natural and man-made surfaces.

These indices were spatially analyzed across growth stages to confirm their correlation with wheat biomass and age.

3.4 Field Data Integration and Grouping

Field measurements were harmonized with decomposition outputs based on acquisition dates. Each SAR acquisition was linked to a specific GT campaign (see Section 2.3). The spatial footprint of GT plots was overlaid on the decomposition raster products using GPS coordinates, and mean pixel values were extracted for each plot. Field data were grouped into three biomass classes and three age classes (Table 2). This stratification allowed statistical comparison across decomposition components, enabling evaluation of their sensitivity and dynamic range.

4. Results

4.1 RH and RV Backscatter versus Biomass and Age

The response of RH and RV backscatter to wheat biomass and age was evaluated using ground truth–linked pixels from all three acquisition dates (Fig. 5). The RH channel exhibited a moderately strong inverse relationship with both crop biomass and age, while the RV channel showed negligible sensitivity possibly due to stronger coupling and attenuation of the vertically polarised signal.

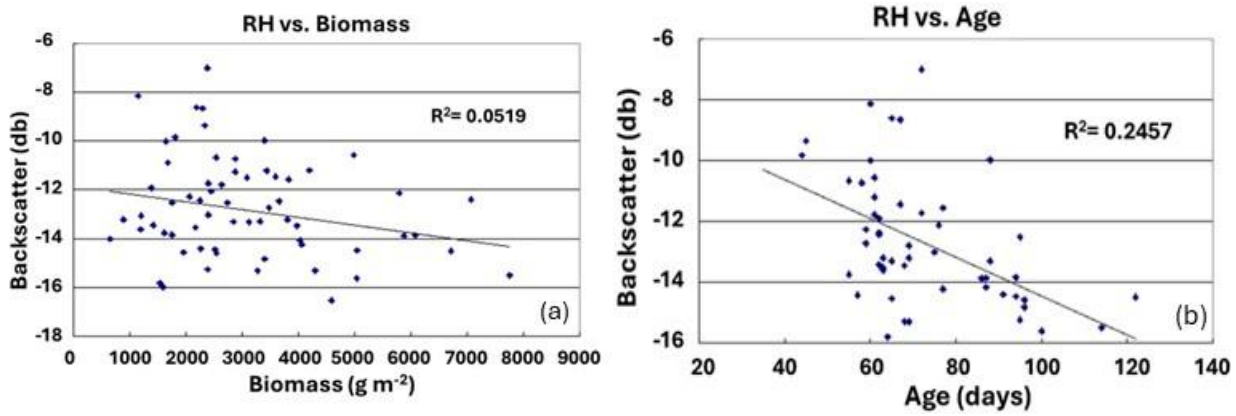


Fig. 5. (a) RH backscatter versus wheat biomass; (b) RH backscatter versus crop age.

RH backscatter values decreased from –8 dB to –13 dB as biomass increased beyond 5000 g/m², consistent with previous findings for erectophile crops like wheat (Raney 2016; Haldar et al. 2017). This trend is attributed to enhanced volume scattering and signal attenuation within the vertical canopy structure. In contrast, RV backscatter remained largely invariant across the same biomass and age ranges, indicating its limited sensitivity for biophysical parameter retrieval in erectophile systems. The weak RV response is attributed to its polarization geometry being less responsive to vertical vegetation structures, corroborating earlier observations in wheat and mustard (Raney 2016).

These trends reaffirm that RH polarization, similar to HH in conventional full-pol SAR systems, offers more diagnostic information for wheat-type canopies, whereas RV (akin to HV) is more suited to planophile crops with horizontally oriented leaves such as mustard, cotton, groundnut and soybean (Haldar et al. 2017).

4.2 Radar Vegetation Index (*RVI*) And Alpha Angle

The Radar Vegetation Index (*RVI*) was calculated from the Stokes parameters for all field plots. *RVI* values ranged from 0.27 in sparse vegetative conditions to 0.52 (moderate range) akin to derived from hybrid-pol data in dense wheat fields (Fig. 6). A clear increasing trend was observed with biomass, while the relationship with crop age was found to be weaker and more scattered.

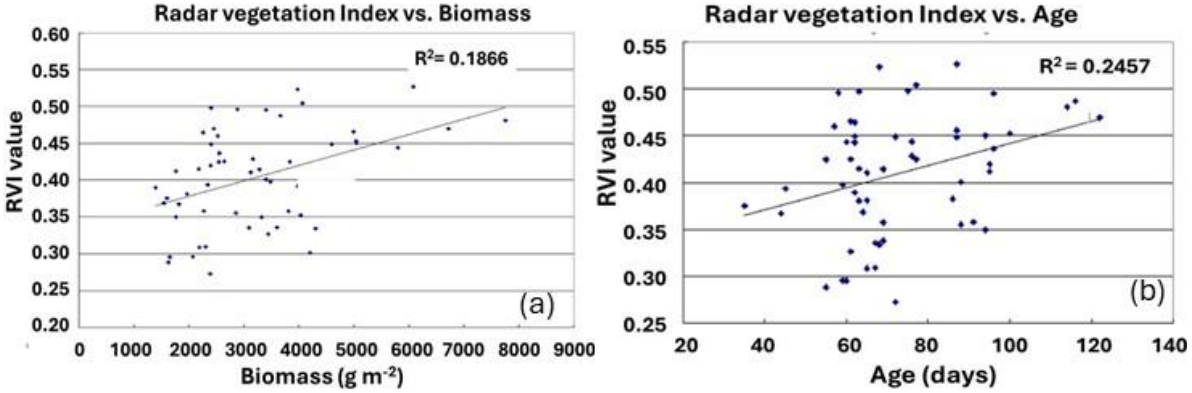


Fig. 6. (a) Radar Vegetation Index (*RVI*) versus biomass; (b) *RVI* versus crop age.

These results support the idea that vegetation density (biomass) directly influences microwave backscatter characteristics, while age alone may not be a reliable proxy, especially under variable irrigation or nutrient stress. Similar behavior was reported by Kim et al. (2012) and confirmed for erectophile crops by Haldar et al. (2017).

The Alpha Angle, derived from both C2 and pseudo-C3 matrices, exhibited a moderate correlation with both biomass and crop age. As shown in Fig. 7, alpha values ranged from approximately 26° to 45°, indicating a transition from surface scattering (low biomass/early stages) < 10 deg to volume (30-45) and dipole scattering (high biomass/mature stages 45-55).

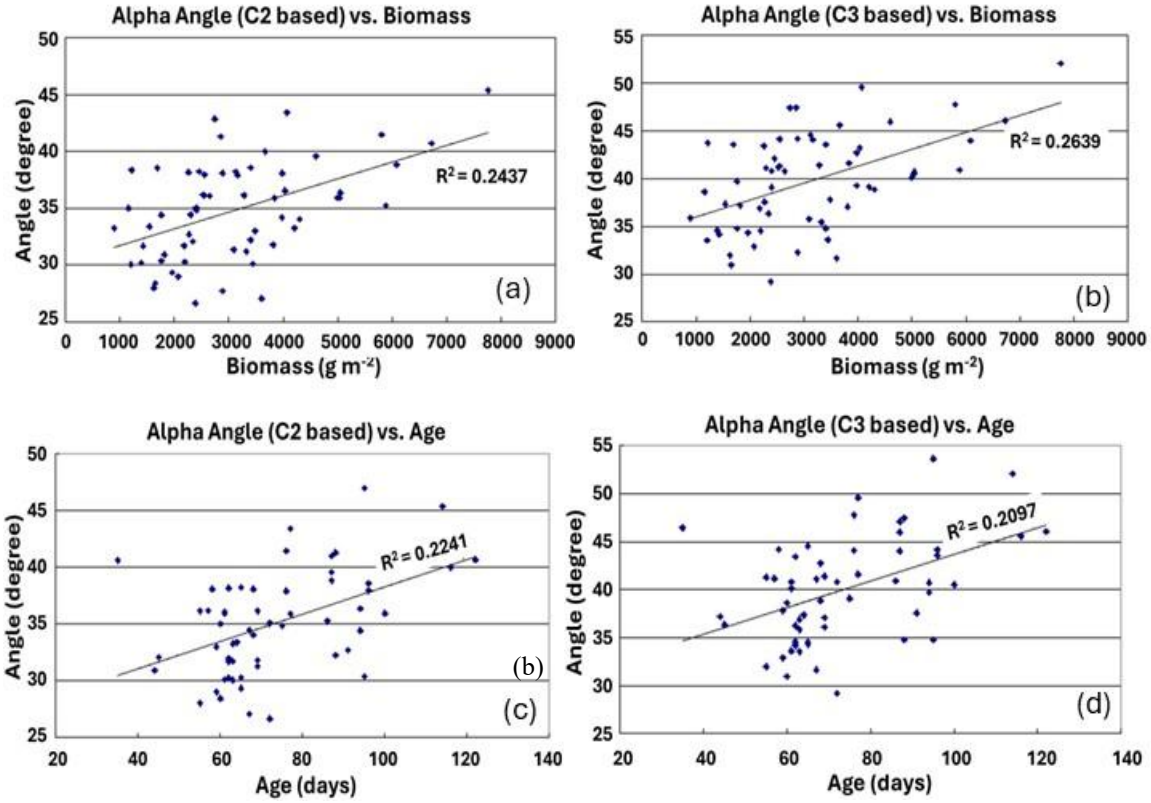


Fig. 7. (a–d) Alpha Angle versus biomass and age from C2 and pseudo-C3 matrices.

The C3-based Alpha Angle showed slightly higher sensitivity, in line with previous studies indicating improved scattering separation in three-component models (Cloude and Pottier 1997; Haldar et al. 2016a) nevertheless C2 based angles performed almost equally well. These trends underscore the physical significance of Alpha Angle characterizing canopy development and structure in cereal crops.

4.3 Stokes Parameter-Based Decomposition

The Stokes-based m-δ and m-χ decompositions were analyzed across stratified biomass and crop age classes. Each decomposition produced three primary components - even, odd, and diffuse corresponding to surface, dihedral, and volumetric scattering, respectively. Mean values of these components, alongside Radar Vegetation Index (*RVI*) and Alpha Angle, were computed for each class and are presented in Table 3 (biomass-wise) and Table 4 (age-wise).

Table 3. Mean decomposition parameters and indices for different biomass classes.

Biomass Range (g m^{-2})	*RVI*	Alpha Angle C2	Alpha Angle C3	m-δ Even	m-δ Diffuse	m-δ Odd
< 2500	0.27	32.6	37.9	0.274	0.367	0.358
2500–5000	0.41	35.7	40.9	0.336	0.396	0.277
> 5000	0.52	39.1	44.6	0.387	0.439	0.257

As seen in Table 3, both *RVI* and Alpha Angle increased with biomass, confirming their suitability for characterizing vegetation density and structure. The *m-δ* diffuse and even component exhibited a strong positive trend with biomass, while the odd component declined significantly indicating reduced surface scattering as the canopy matured. These trends are visualized in Fig. 8, which further illustrates the smooth separation of scattering contributions across biomass classes. The *δ* angle being the phase difference between the *RH* and *RV* channel bringing out the co-pol phase difference essence of the target.

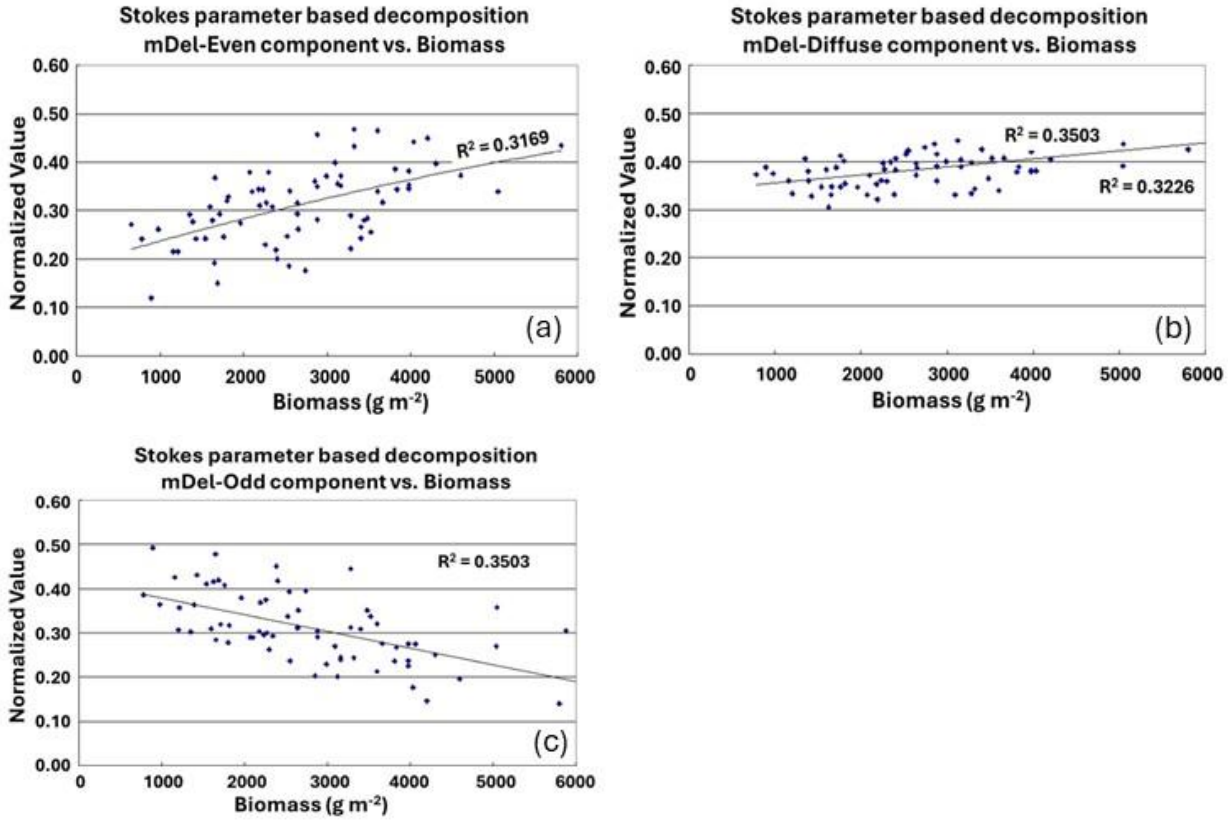


Fig. 8**.** (a) Even, (b) Diffuse and (c) Odd m-δ decomposition components versus biomass

To examine temporal behavior, the same analysis was applied to age-based crop groups. Results are summarized in Table 4.

Table 4. Mean decomposition parameters and indices for different age classes.

Crop Age (days)	*RVI*	Alpha Angle C2	Alpha Angle C3	m-δ Even	m-δ Diffuse	m-δ Odd
< 70	0.393	33.1	37.8	0.297	0.365	0.339
70–105	0.427	37.0	42.2	0.318	0.410	0.278
> 105	0.479	42.0	47.9	0.292	0.435	0.274

In Table 4, Alpha Angle values confirmed a transition from surface to volume-dominant scattering with age. The m-δ diffuse component increased with crop maturity, while the odd component declined, similar to biomass-based grouping. These patterns are clearly shown in Fig. 9. The odd-bounce component shows a relatively high data spread across biomass and age classes. The double-bounce scattering component exhibits an increasing trend with crop development, while the volume scattering component increases progressively across growth stages. A corresponding increase in the Alpha Angle is observed with increasing biomass and
crop age.

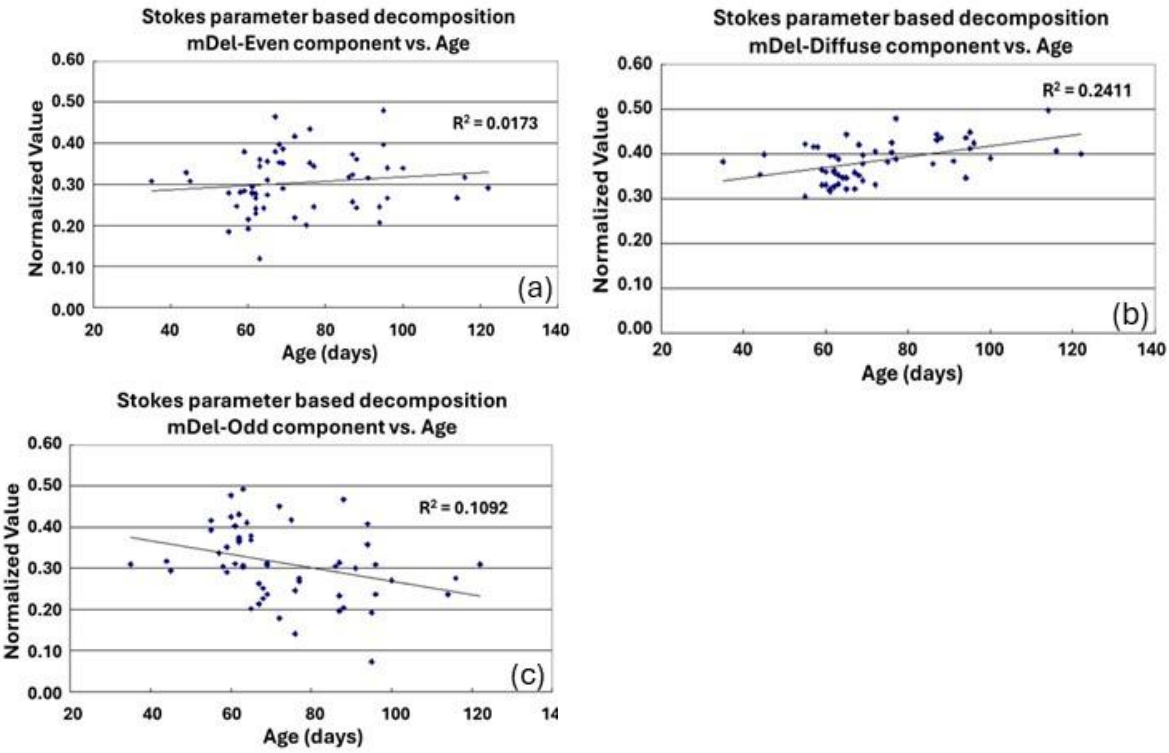


Fig. 9. (a) Even, (b) Diffuse and (c) Odd m-δ decomposition components versus crop age.

For comparison, m-χ decomposition was evaluated across the same groupings. While component trends were similar, the dynamic range was lower and statistical separation across classes was weaker, indicating lower biophysical sensitivity than m-δ. These comparative behaviors are illustrated in Fig. 10 and 11.

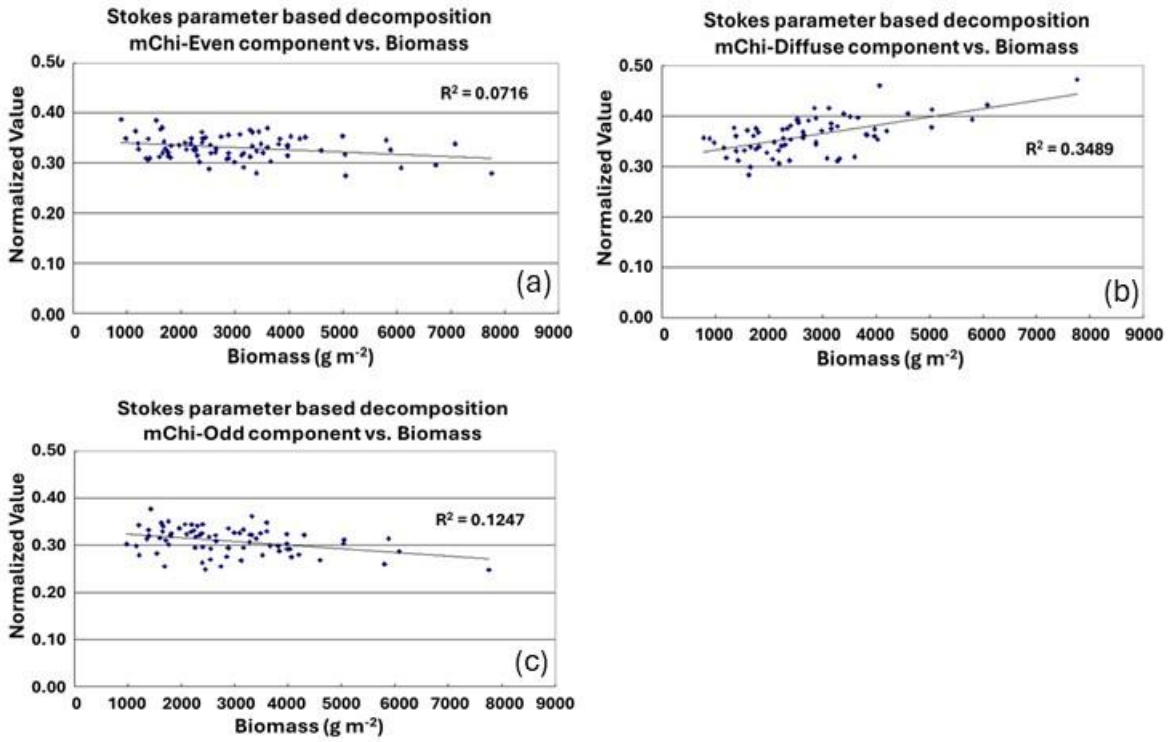


Fig. 10**.** (a) Even, (b) Diffuse and (c) Odd m-χ decomposition components versus biomass.

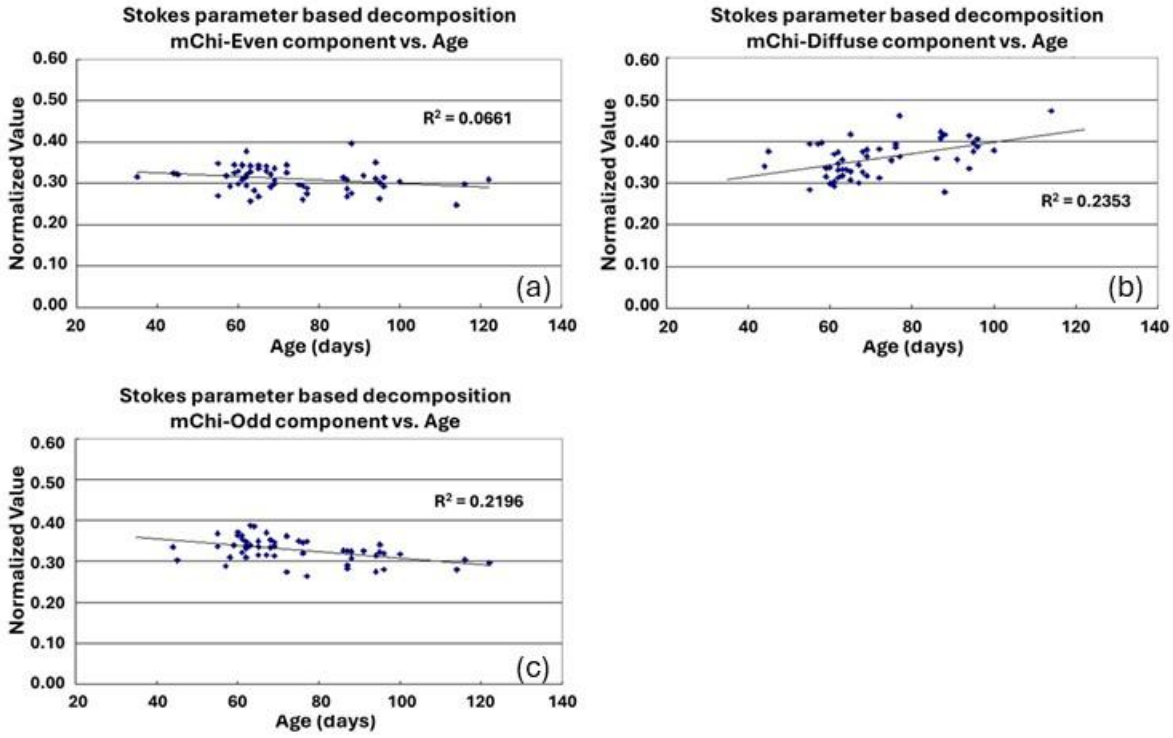


Fig. 11. (a) Even, (b) Diffuse and (c) Odd m-χ decomposition components versus crop age.

A cross-method comparison was performed to benchmark the volume (diffuse) component obtained from m-δ, m-χ, Raney decomposition, and a multilooked version of m-δ. As shown in Fig. 12, the m-δ full-resolution decomposition clearly outperformed others, with higher correlation to biomass and wider dynamic spread. The Raney and multilooked outputs showed flatter responses and reduced sensitivity, reinforcing the utility of full-resolution Stokes-based decomposition for field-scale precision crop monitoring.

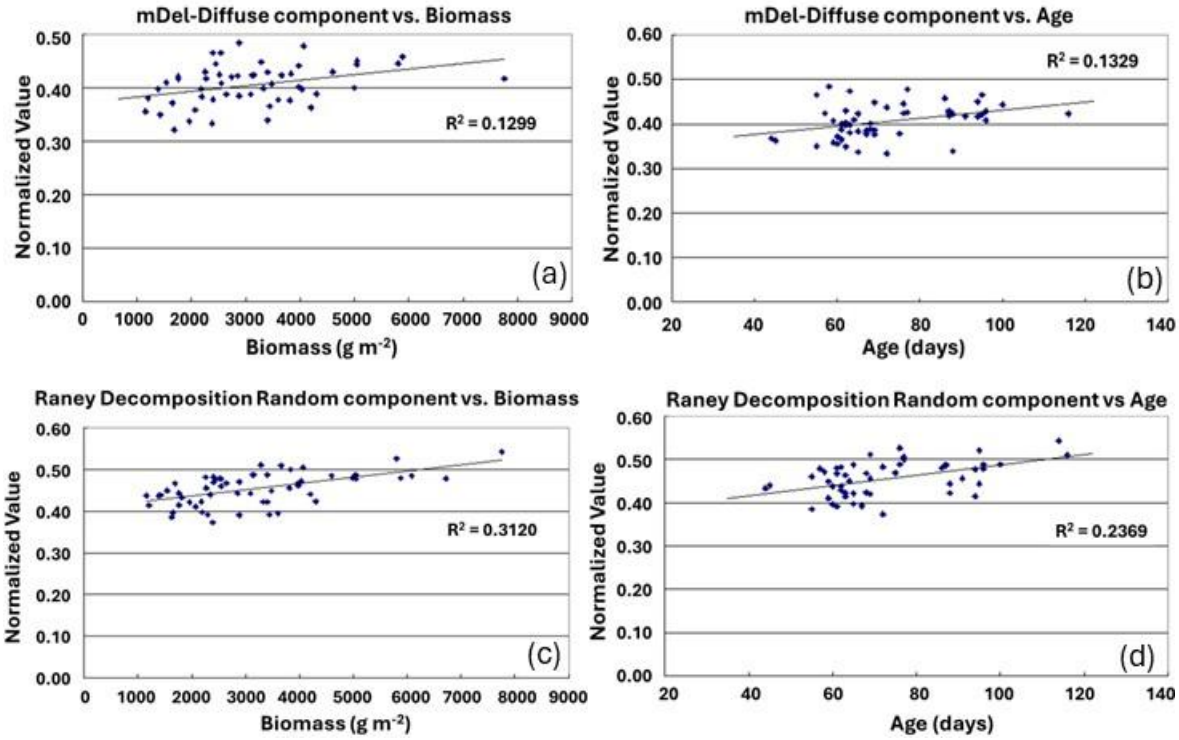


Fig. 12. Comparison of volume scattering (diffuse) component from m-δ, and Raney decompositions versus biomass and age.

The tables and figure-based analyses confirm that m-δ decomposition provides the most interpretable and responsive scattering signature, supporting its application for biomass and phenological stage retrieval, better than dual-pol based entropy (Haldar et al. 2021) in operational wheat monitoring.

4.4 Comparison with Raney and Multilooked Decompositions

To benchmark the performance of Stokes parameter–based methods, a comparative analysis was conducted using Raney decomposition and multilooked m-δ decomposition derived in PolSARpro (Fig. 12).

Key comparisons:

- The volume component from m-δ showed the strongest positive correlation with biomass ($R^2 > 0.4$), followed by m-χ.
- The Raney decomposition exhibited the least dynamic response, with volume component saturating at ~0.5 and R^2 values below 0.2.

- Multilooked outputs showed reduced sensitivity due to speckle averaging and smoothing, reaffirming the advantage of using full-resolution decomposition for fine-scale crop biophysics.

Overall, m-δ decomposition outperformed the others in terms of both statistical strength and interpretability. The results validate earlier findings by Raney (Chirakkal et al. 2019) and expand them to show that Stokes-based m-δ decomposition is more robust for natural ecosystem agricultural targets, particularly under variable canopy conditions.

5. Discussion

The results presented in this study demonstrate the superior sensitivity and physical interpretability of the m-δ decomposition derived from Stokes parameters for retrieving wheat biophysical parameters using hybrid polarimetric SAR data. The consistent trends in component behavior, particularly the strong inverse relation of odd bounce with biomass and age, and the increasing contribution of the diffuse component highlight the ability of m-δ to capture the structural evolution of wheat canopies across phenological growth stages.

Compared to m-χ decomposition, m-δ exhibits a more stable and interpretable response across vegetation growth classes. This is due to m-δ's reliance on intensity-based separation using S_1 (related to polarization anisotropy) and co-pol phase difference essence from the partial polarimetry, whereas m-χ integrates phase-based behavior through the ellipticity of the polarization ellipse (Raney 2024; Chirakkal et al. 2017). While m-χ offers useful geometrical interpretations in depolarizing or natural targets such as forests (Thota et al. 2025), its application in agricultural settings has been shown to be less robust due to weaker separation between canopy and surface scattering under changing moisture and tillage conditions added to slower growth of some crops in the initial one month. (Chirakkal et al. 2017; Abdikan et al. 2018).

Although Raney decomposition conceptually encompasses elements of other hybrid polarimetric decompositions and is specifically designed for compact and hybrid SAR systems, it exhibited reduced sensitivity in this study. The diffuse and odd scattering components derived from Raney decomposition showed relatively flat responses across biomass classes, indicating limited capability for capturing subtle canopy structural variations in erectophile crops. These findings agree with earlier observations made using compact polarimetric datasets over cotton, maize and rice (Bouvet et al. 2009), where Raney decomposition captured general trends but lacked the fine dynamic range needed for field-level biophysical monitoring. Additionally, the multilooked Raney outputs, processed in PolSARpro, showed lower correlation coefficients ($R^2 < 0.2$) compared to full-resolution m-δ results ($R^2 > 0.4$), reaffirming the importance of preserving full-resolution Stokes parameter data when analyzing smallholder plots or heterogeneous cropping patterns.

In contrast, the m-δ decomposition components map clearly onto crop structural evolution:

- The odd component, linked to surface scattering, is dominant in early growth stages when the soil is partially exposed. Its steady decline with increasing age and biomass is consistent with vegetation-induced attenuation of surface returns.
- The diffuse component, attributed to volume scattering, increases steadily as the crop canopy becomes denser, directly linked to increase in the relative number of scattering elements and more vertically layered, a behavior well documented in SAR studies on cotton, corn, rice, and wheat (Charbonneau et al. 2010; Kim et al. 2012; Cloude et al. 2012).
- The even component shows moderate growth, consistent with the development of double-bounce structures between erect stems arranged in definite rows and the soil surface.

These component-level behaviors validate theoretical expectations from physical scattering models such as the Freeman–Durden and Cloude–Pottier decompositions (Cloude and Pottier 1997), (Vreugdenhil et al. 2018), adapted here for hybrid/compact-polarimetric data. The benefit of using Stokes-based decompositions lies in avoiding the need to reconstruct full covariance or coherency matrices, making this method ideal for hybrid-polarity SAR like RISAT-1 and RISAT-1A (Raney 2007a), (Chirakkal et al. 2019).

From a crop physiology perspective, these findings align with earlier dual-pol SAR studies in India in which significant HH and HV backscatter variability for wheat and mustard during biomass accumulation stages was observed (Haldar et al. 2012; Haldar et al. 2016b; Haldar et al. 2017). These studies also reported limited HV sensitivity for erectophile crops, due to low depolarization from vertical canopy structures. Our observations on the limited RV response further confirm this behavior. Although HV represents a partial response of the RV channel, with RV containing contributions from both horizontal and vertical polarizations (RV = (H+V) V), HV may be treated as a surrogate for RV. However, unlike pure cross-polarized returns, HV also includes coupled co-polarized scattering contributions. In contrast, planophile crops such as cotton, with broad horizontal leaves, demonstrate enhanced HV or RV scattering due to increased volume–surface coupling (Maity et al. 2004; Abdikan et al. 2018).

In terms of operational implications, the validated sensitivity of m-δ decomposition parameters—especially the diffuse component offers a strong case for integrating hybrid SAR into routine crop monitoring workflows, particularly in countries where full-polarimetric coverage is scarce. The reintroduction of hybrid capability through RISAT-1A offers new possibilities for national-scale agricultural applications, including pre-sowing condition assessments, in-season growth monitoring/crop-condition assessment, and yield estimation and multiple crop monitoring studies are in progress nationally.

The low-cost, single-channel transmit design of hybrid systems allows broader swath and revisit cycles, which are critical for operational programs like FASAL-2 (Forecasting Agricultural output using Space, Agro-meteorology and Land-based observations), Sustainable Use of Farm Assets for Livelihood Advancement and Management (SUFALAM), Joint Experiment on Crop Assessment and Monitoring (JECAM), and various other crop monitoring programs. The results of this study may help optimize sensor tasking and algorithm development for such operational settings.

Importantly, the statistical stratification into biomass and age groups, validated using in-situ field data, enhances the robustness of decomposition sensitivity analysis. Studies relying solely on backscatter–biomass regression often struggle with confounding factors such as soil moisture and crop health variability (McNairn and Shang 2016; Haldar et al. 2021). By pairing decomposition outputs with physically grounded scattering indicators like Alpha Angle and Radar Vegetation Index (*RVI*), this study proposes a multi-parametric framework that improves retrieval confidence.

The Alpha Angle, in particular, showed increasing values with crop maturity, indicative of a shift from surface to volume scattering regimes. The pseudo-C3-derived Alpha Angle showed higher sensitivity than the C2-based one, supporting previous findings (Cloude and Pottier 1997; Charbonneau et al. 2010), who emphasized the benefits of pseudo full-pol approximations for capturing complex canopy interactions. Similarly, the *RVI* values ranging from 0.27 to 0.52 fell within expected ranges for wheat in semi-arid systems (Charbonneau et al. 2010; Kim et al. 2012) and provide a normalized measure of vegetation vigor that can complement decomposition-based estimates.

Beyond India, the results of this study hold value for hybrid or compact SAR systems operated by other space agencies. Missions like SAOCOM-1A (Argentina), RCM (Canada), ALOS-3 (Japan), and the

current NISAR in-orbit (NASA–ISRO) mission can benefit from the decomposition framework guided crop monitoring demonstrated here. As demonstrated by Haldar et al. (2021) and Thota et al. (2025), hybrid polarimetric decomposition approaches such as m-δ exhibit transferable physical interpretation across L-, C-, and S-band SAR systems, provided that differences in spatial resolution and polarimetric calibration are appropriately accounted for.

The scalability of these methods for cloud computing platforms such as Google Earth Engine, SNAP, or ISRO's Bhuvan services further enhances their practical relevance. With time-series stack support, the diffuse component from m-δ can serve as a biomass growth tracker, while *RVI* trends may inform drought stress or irrigation timing. This becomes particularly relevant in climate-sensitive regions where intra-seasonal variability affects sowing decisions—as observed in this study's 2016 drought year, when wheat acreage declined significantly and cumin/coriander replaced traditional cereal crops (Haldar et al. 2017).

Still, certain limitations warrant consideration. First, the spatial transferability of decomposition thresholds (e.g., diffuse > 0.4 indicating high biomass) remains context dependent. Calibration across soil types, crop types and varieties, and management practices are necessary. Second, hybrid polarimetric SAR lacks sensitivity to biochemical traits such as chlorophyll content or nutrient stress, which might precede canopy structure changes. Studies integrating SAR–optical fusion (e.g., Sentinel-1 + Sentinel-2) (Veloso et al. 2017) and hyperspectral- SAR coupling (Yao et al. 2022) have been used for synergistic understanding of the biochemical and physiological processes or thermal–SAR synergy for early stress detection (Jiao et al. 2022)

Finally, while this study emphasizes *m-δ* for wheat, extending its application to multi-cropping systems, horticultural crops, or mixed orchards will require customized training datasets and possibly defining different decomposition thresholds for these ecosystems. Incorporating machine learning–based classification of decomposition outputs could aid in this direction, especially under supervised frameworks (Thota et al. 2025; Jiao et al. 2022).

While the study demonstrates the effectiveness of Stokes parameter-based hybrid polarimetric decompositions for wheat biophysical parameter retrieval, certain limitations must be acknowledged. First, the temporal coverage was constrained by the availability of suitable RISAT-1 acquisitions, especially due to varying viewing geometries across ascending and descending orbits. This limited the continuity of phenological monitoring and hindered pixel-level multi-temporal consistency.

Second, although the decomposition techniques showed strong correlation with crop biomass and age under the semi-arid agroclimatic conditions of Junagadh, their spatial transferability across diverse soil types, irrigation regimes, and wheat cultivars remains to be validated. Similar hybrid and fully polarimetric SAR approaches have been applied to other semi-arid crops, such as pearl millet, using RADARSAT-2 and RISAT-1A data. In north Indian scenario (Haryana), decomposition-based classification has been successfully used (Chirakkal et al. 2019). Calibration and threshold refinement across different agroecological zones will be essential for national-scale operational deployment.

Third, while the *m-δ* decomposition performed robustly in this study, the integration of machine learning algorithms could further enhance the interpretability and automation of biophysical retrieval by learning complex, non-linear patterns across decomposition parameters and vegetation indices. This is particularly relevant in heterogeneous cropping systems and mixed land cover scenarios where rule-based decomposition thresholds may be insufficient.

Future work should explore SAR-hyperspectral data fusion and multi-sensor integration (e.g., Sentinel-1/2, RISAT-1A) for early stress detection and multi-crop monitoring, as well as development of time-series biomass tracking using the m-δ diffuse component. Additionally, incorporation of cloud-based

analytics (e.g., Google Earth Engine) can facilitate scalable implementation for real-time agricultural decision support.

This study demonstrates the efficacy of hybrid polarimetric SAR data, particularly RISAT-1, in retrieving biophysical parameters of wheat through the application of Stokes parameter–based decomposition techniques. Among the decomposition methods evaluated, the m-δ decomposition consistently outperformed both m-χ and Raney decompositions in terms of dynamic sensitivity and correlation with ground-based biomass (field scale validation) and crop age observations. The diffuse component derived from m-δ decomposition emerged as a reliable indicator of canopy development, increasing steadily with crop maturity and biomass. Conversely, the odd component exhibited a decreasing trend, indicating the diminishing influence of surface scattering as the canopy closed. The Radar Vegetation Index (*RVI*) and Alpha Angle further reinforced these patterns, confirming their utility as ancillary biophysical proxies when used in conjunction with decomposition parameters.

6. Conclusions

The findings validate the applicability of hybrid SAR data for crop structural monitoring, particularly in erectophile crops like wheat where traditional cross-polarized responses are weak. Other cereal crops, such as millets, are expected to gain importance under climate change scenarios and may replace traditional cereals across many tropical and subtropical regions. The approach developed in this study can be extended to these crops, supporting future efforts toward global nutritional security. The hybrid decomposition framework presented here offers a robust, operationally feasible alternative to full-polarimetric approaches, especially valuable for missions like RISAT-1A, which provides hybrid polarimetry with improved temporal resolution. Beyond methodological insights, this work provides a transferable decomposition strategy compatible with hybrid and compact polarimetric data from multiple platforms. The use of in situ field data for validation enhances the robustness of the approach and supports its potential integration into field-scale, village level national crop monitoring systems focusing on kharif season inputs in precision farming, particularly in data-sparse, cloud-prone environments.

Future research could extend this framework to additional crop types, incorporate SAR–optical fusion, and explore machine learning integration to automate decomposition-driven biophysical retrieval at scale. As the demand for high-resolution, near-real-time crop monitoring grows, hybrid polarimetric SAR, supported by rigorous decomposition methods, will be pivotal in advancing precision agriculture and food security planning.

Statements and Declarations

Funding: This work was supported by the Indian Space Research Organisation under the RISAT Utilization Programme through the Space Applications Centre, Ahmedabad.

Competing Interests: The authors declare that they have no financial or non-financial interests that are directly or indirectly related to the work submitted for publication.

Data Availability: The data supporting the findings of this study are available from the corresponding author upon reasonable request, subject to the data-sharing policies of the Indian Space Research Organisation.

Code Availability: The processing codes used in this study are available from the corresponding author upon reasonable request, subject to institutional data- and code-sharing policies.

References:

Abdikan S, Sekertekin A, Ustunern M, Balik Sanli F, Nasirzadehdizaji R (2018) Backscatter analysis using multi-temporal Sentinel-1 SAR data for crop growth of maize in Konya Basin, Turkey. Int Arch Photogramm Remote Sens Spatial Inf Sci XLII-3:9–13. https://doi.org/10.5194/isprs-archives-XLII-3-9-2018

Bouvet A, Le Toan T, Lam-Dao N (2009) Monitoring of the rice cropping system in the Mekong Delta using ENVISAT/ASAR dual-polarization data. IEEE Trans Geosci Remote Sens 47:517–526. https://doi.org/10.1109/TGRS.2008.2007963

Charbonneau FJ, Brisco B, Raney RK, McNairn H, Liu C, Vachon P, Shang J, DeAbreu R, Champagne C, Merzouki A, Geldsetzer T (2010) Compact polarimetry overview and applications assessment. Can J Remote Sens 36(Suppl 2):S298–S315. https://doi.org/10.5589/m10-062

Chirakkal S, Haldar D, Misra A (2017) Evaluation of hybrid polarimetric decomposition techniques for winter crop discrimination. Prog Electromagn Res M 55:73–84. https://doi.org/10.2528/PIERM17011603

Chirakkal S, Haldar D, Misra A (2019) A knowledge-based approach for discriminating multi-crop scenarios using multi-temporal polarimetric SAR parameters. Int J Remote Sens 40:4002–4018. https://doi.org/10.1080/01431161.2018.1558304

Cloude SR, Goodenough DG, Chen H (2012) Compact decomposition theory. IEEE Geosci Remote Sens Lett 9:28–32. https://doi.org/10.1109/LGRS.2011.2158983

Cloude SR, Pottier E (1997) An entropy-based classification scheme for land applications of polarimetric SAR. IEEE Trans Geosci Remote Sens 35:68–78. https://doi.org/10.1109/36.551935

European Space Agency (2015) PolSARpro v5.0: polarimetric SAR data processing and educational tool: user guide. ESA. https://earth.esa.int/eogateway/tools/polsarpro. Accessed on 8th Aug 2026.

FAO, IFAD, UNICEF, WFP, WHO (2025) The state of food security and nutrition in the world 2025: addressing high food price inflation for food security and nutrition. FAO, Rome. https://doi.org/10.4060/cd6008en

Freeman A, Durden SL (1998) A three-component scattering model for polarimetric SAR data. IEEE Trans Geosci Remote Sens 36:963–973. https://doi.org/10.1109/36.673687

Haldar D et al (2017) RISAT hybrid data analysis for kharif crops: analysis report for 2015 datasets. Technical Report SAC/EPSA/GHCAG/MHTD/TR-02, Space Applications Centre, Indian Space Research Organisation, Ahmedabad

Haldar D, Das A, Mohan S, Pal O, Hooda RS, Chakraborty M (2012) Assessment of L-band SAR data at different polarization combinations for crop and other landuse classification. Prog Electromagn Res B 36:303–321. https://doi.org/10.2528/PIERB11071106

Haldar D, Dave V, Dave R, Pandey V, Misra A (2016a) RISAT hybrid data analysis for rabi crops: analysis report for 2015 datasets. Technical Report SAC/EPSA/GHCAG/MHTD/TR-09, Space Applications Centre, Indian Space Research Organisation, Ahmedabad

Haldar D, Rana P, Yadav M, Hooda RS, Chakraborty M (2016b) Time series analysis of co-polarization phase difference (PPD) for winter field crops using polarimetric C-band SAR data. Int J Remote Sens 37:3753–3770. https://doi.org/10.1080/01431161.2016.1204024

Haldar D, Verma A, Kumar S, Chauhan P (2021) Estimation of mustard and wheat phenology using multi-date Shannon entropy and radar vegetation index from polarimetric Sentinel-1. Geocarto Int 37:5935–5962. https://doi.org/10.1080/10106049.2021.1926554

Inglada J, Vincent A, Arias M, Tardy B, Morin D, Rodes I (2017) Operational high-resolution land cover map production at the country scale using satellite image time series. Remote Sens 9:95. https://doi.org/10.3390/rs9010095

ISRO (2025) RISAT-1 mission. Indian Space Research Organisation. https://www.isro.gov.in/RISAT_1.html. Accessed January 2026

Jiao X, McNairn H, Yekkehkhany B, Dingle Robertson L, Ihuoma S (2022) Integrating Sentinel-1 SAR and Sentinel-2 optical imagery with a crop structure dynamics model to track crop condition. Int J Remote Sens 43:6509–6537. https://doi.org/10.1080/01431161.2022.2142077

Kim Y, Jackson T, Bindlish R, Lee H, Hong S (2012) Radar vegetation index for estimating the vegetation water content of rice and soybean. IEEE Geosci Remote Sens Lett 9:564–568. https://doi.org/10.1109/LGRS.2011.2174772

Maity M, Patnaik C, Panigrahy S (2004) Analysis of temporal backscattering of cotton crops using a semi-empirical model. IEEE Trans Geosci Remote Sens 42:577–587. https://doi.org/10.1109/TGRS.2003.821888

McNairn H, Shang J (2016) A review of multitemporal synthetic aperture radar (SAR) for crop monitoring. In: Ban Y (ed) Multitemporal remote sensing. Springer, Cham, pp 317–336. https://doi.org/10.1007/978-3-319-47037-5_15

Raney RK (2007a) Hybrid-polarity SAR architecture. IEEE Trans Geosci Remote Sens 45:3397–3404. https://doi.org/10.1109/TGRS.2007.895883

Raney RK (2007b) Decomposition of hybrid-polarity SAR data. In: Lacoste H, Ouwehand L (eds) Proceedings of the 3rd International Workshop on Science and Applications of SAR Polarimetry and Polarimetric Interferometry (PolInSAR 2007), 22–26 January 2007, Frascati, Italy. ESA Publications, ESTEC, Noordwijk, SP-644

Raney RK (2016) Comparing compact and quadrature polarimetric SAR performance. IEEE Geosci Remote Sens Lett 13:861–864. https://doi.org/10.1109/LGRS.2016.2550863

Raney RK (2024) Radar polarimetry: classical versus quad-pol methodologies. IEEE Geosci Remote Sens Lett 21:1–5. https://doi.org/10.1109/LGRS.2024.3352987

Singha C, Swain KC (2023) Rice crop growth monitoring with Sentinel-1 SAR data using machine learning models in Google Earth Engine cloud. Remote Sens Appl Soc Environ 32:101029. https://doi.org/10.1016/j.rsase.2023.101029

Skriver H, Svendsen MT, Thomsen AG (1999) Multitemporal C- and L-band polarimetric signatures of crops. IEEE Trans Geosci Remote Sens 37:2413–2429. https://doi.org/10.1109/36.789639

Song XP, Huang W, Hansen MC, Potapov P (2021) An evaluation of Landsat, Sentinel-2, Sentinel-1 and MODIS data for crop type mapping. Sci Remote Sens 3:100018. https://doi.org/10.1016/j.srs.2021.100018

Thota S, Srivastava HS, Kumar D (2025) Comparative evaluation of hybrid polarimetric decomposition techniques for land-cover mapping. Int J Space Appl 1(1). https://www.ijsa-prp.in

Thota S, Srivastava HS, Sharma PK, Dhiraj K, Patel P (2015) Study of hybrid polarimetric parameters generated from RISAT-1 SAR data for various land-cover targets. Int J Adv Remote Sens GIS Geogr 3:32–42

Veloso A, Mermoz S, Bouvet A, Le Toan T, Planells M, Dejoux JF, Ceschia E (2017) Understanding the temporal behavior of crops using Sentinel-1 and Sentinel-2-like data for agricultural applications. Remote Sens Environ 199:415–426. https://doi.org/10.1016/j.rse.2017.07.015

Vreugdenhil M, Wagner W, Bauer-Marschallinger B, Pfeil I, Teubner I, Rüdiger C, Strauss P (2018) Sensitivity of Sentinel-1 backscatter to vegetation dynamics: an Austrian case study. Remote Sens 10:1396. https://doi.org/10.3390/rs10091396

Yao H, Fu B, Zhang Y, Li S, Xie S, Qin J, Fan D, Gao E (2022) Combination of hyperspectral and quad-polarization SAR images to classify marsh vegetation using stacking ensemble learning algorithm. Remote Sens 14:5478. https://doi.org/10.3390/rs14215478